

## Spin-orbit-induced mixed-spin ground state in $R\text{NiO}_3$ perovskites probed by x-ray absorption spectroscopy: Insight into the metal-to-insulator transition

C. Piamonteze,<sup>1,2</sup> F. M. F. de Groot,<sup>3</sup> H. C. N. Tolentino,<sup>1</sup> A. Y. Ramos,<sup>1,4</sup> N. E. Massa,<sup>5</sup>  
J. A. Alonso,<sup>6</sup> and M. J. Martínez-Lope<sup>6</sup>

<sup>1</sup>Laboratório Nacional de Luz Síncrotron, Caixa Postal 6192, 13084-971, Campinas, São Paulo, Brazil

<sup>2</sup>IFGW/UNICAMP, 13083-970, Campinas, São Paulo, Brazil

<sup>3</sup>Department of Inorganic Chemistry and Catalysis, Utrecht University, Sorbonnelaan 16, 3584 CA, Utrecht, The Netherlands

<sup>4</sup>LMCP-CNRS, Université de Paris 6, Paris, France

<sup>5</sup>Laboratorio Nacional de Investigación y Servicios en Espectroscopía Óptica, Centro CEQUINOR, UNLP, 1900 La Plata, Argentina

<sup>6</sup>Instituto de Ciencia de Materiales de Madrid, C.S.I.C., Cantoblanco, E-28049 Madrid, Spain

(Received 17 June 2004; revised manuscript received 5 November 2004; published 26 January 2005)

We report on a Ni  $L_{2,3}$  edge x-ray absorption spectroscopy study in  $R\text{NiO}_3$  perovskites. These compounds exhibit a metal-to-insulator (MI) transition as temperature decreases. The  $L_3$  edge presents a clear splitting in the insulating state, associated to a less hybridized ground state. Using charge transfer multiplet calculations, we establish the importance of the crystal field and  $3d$  spin-orbit coupling to create a mixed-spin ground state. We explain the MI transition in  $R\text{NiO}_3$  perovskites in terms of modifications in the  $\text{Ni}^{3+}$  crystal field splitting that induces a spin transition from an essentially low-spin to a mixed-spin state.

DOI: 10.1103/PhysRevB.71.020406

PACS number(s): 75.10.Dg, 75.25.+z, 78.70.Dm, 71.30.+h

Rare-earth nickel perovskites ( $R\text{NiO}_3$ ,  $R$ =rare earth) present a sharp well-defined metal-to-insulator (MI) transition as temperature decreases.<sup>1</sup> The transition temperature,  $T_{\text{MI}}$ , increases with reducing the  $R$  ion size, which determines the degree of distortion of the structure.<sup>2</sup> It was proposed that the gap opening would be due to a smaller Ni-O-Ni superexchange angle leading to a reduction of the bandwidth.<sup>3</sup> However, non-negligible electron-phonon interactions<sup>4</sup> and a shift in  $T_{\text{MI}}$  with oxygen isotope substitution<sup>5</sup> evidenced the importance of modifications in Ni-O interatomic distances, suggesting a phonon-assisted mechanism for conduction. As temperature decreases, these nickelates undergo a magnetic transition to an unusual antiferromagnetic order.<sup>6-8</sup> The magnetic arrangement for the lighter  $R$  compounds ( $R$ =Pr, Nd, Sm, Eu) was refined with a single Ni moment ( $0.9 \mu_B$ ) and required nonequivalent couplings among Ni ions to stabilize the structure.<sup>6,7</sup> This is a quite unusual situation in an orthorhombic crystallographic structure whose Ni sites are all equivalent.<sup>2</sup> For the heavier  $R$  compounds, Alonso *et al.*<sup>8,9</sup> established a monoclinic distortion in the crystallographic structure, leading to two different Ni sites with longer and shorter Ni—O distances alternating along the three axes. The antiferromagnetic structure was explained by a charge ordering defined among the different Ni sites, each one with different magnetic moments ( $1.4$  and  $0.7 \mu_B$  for  $\text{YNiO}_3$ ).<sup>8</sup> More recently, some evidences that the low-temperature distortion is shared by all members of the  $R\text{NiO}_3$  family were reported.<sup>10</sup> Concerning the Ni local structure, our recent extended x-ray absorption fine structure (EXAFS) results demonstrated the existence of two different Ni sites in all  $R\text{NiO}_3$  compounds, regardless of their long-range crystallographic structure.<sup>11,12</sup>

From spectroscopic data together with configuration interaction calculations, Mizokawa *et al.*<sup>13</sup> established for  $\text{PrNiO}_3$  at room temperature a metallic ground state composed of  $34\% 3d^7 + 56\% 3d^8 \underline{L} + 10\% 3d^9 \underline{L}^2$ , where  $\underline{L}$  stands for a

ligand hole. Owing to the high degree of hybridization in the ground state, with hole transfer from Ni  $3d$  to O  $2p$  orbitals, these compounds have been classified as self-doped Mott insulators.<sup>14</sup> Such a mixed metallic ground state, mostly  $-3d^8 \underline{L}$ , is compatible with a  $\text{Ni}^{3+}$  low-spin configuration, because the amount of charge transfer for parallel spin almost equals that for antiparallel spin.<sup>13</sup> However, the spectral shape in  $R\text{NiO}_3$  compounds is very sensitive to the transition from metallic to insulating states<sup>15</sup> and a complete description of the spin degree of freedom remains to be given. As in recent outcomes on  $\text{Co}^{3+}$  oxides,<sup>16,17</sup> where unconventional spin states exist due to the competition between crystal field splitting and effective  $3d$  exchange interaction, assignments made so far about  $\text{Ni}^{3+}$  in  $R\text{NiO}_3$  compounds have to be reexamined.

We report here Ni  $L$  edge absorption measurements, which probes directly the available Ni  $3d$  states, together with charge transfer multiplet calculations. We establish the importance of the crystal field and  $3d$  spin-orbit ( $l \cdot s$ ) coupling to create a mixed-spin ground state. We explain the MI transition in  $R\text{NiO}_3$  perovskites in terms of modifications in the  $\text{Ni}^{3+}$  crystal field splitting that localizes the electronic states and induces a spin transition from an essentially low-spin (LS) to a mixed-spin state, with a quite large contribution from a high-spin (HS) state.

Soft x-ray absorption measurements at the Ni  $L_{2,3}$  edges were carried out at the spherical grating monochromator (SGM) beamline of Laboratório Nacional de Luz Síncrotron (LNLS), Brazil, using a spherical grating monochromator with an energy resolution of  $0.8 \text{ eV}$  at  $845 \text{ eV}$ . Data were collected at  $300$  and  $96 \text{ K}$  using a liquid-nitrogen cold finger. The bulk polycrystalline  $R\text{NiO}_3$  ( $R$ =Pr, Nd, Eu, Y, and Lu) samples were obtained by a wet-chemistry technique, as described elsewhere.<sup>18</sup> The experimental spectra measured at  $300 \text{ K}$  for  $\text{LuNiO}_3$ ,  $\text{YNiO}_3$ ,  $\text{EuNiO}_3$ ,  $\text{NdNiO}_3$ , and  $\text{PrNiO}_3$  are shown in Fig. 1. The MI transition for these compounds

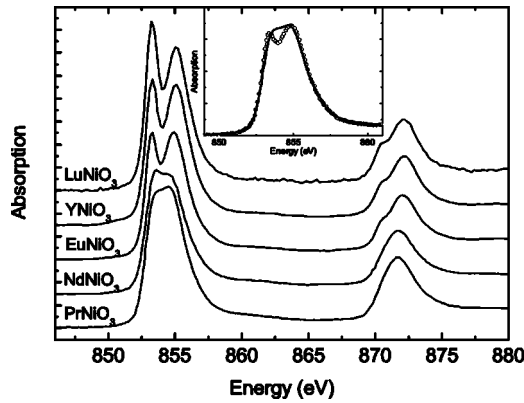


FIG. 1. Ni  $L_{2,3}$  edge spectra at 300 K for PrNiO<sub>3</sub>, NdNiO<sub>3</sub>, EuNiO<sub>3</sub>, YNiO<sub>3</sub>, and LuNiO<sub>3</sub>, whose  $T_{MI}$  are 130, 200, 462, 582 and 599 K, respectively. Inset:  $L_3$  edge spectra for PrNiO<sub>3</sub> at 300 K (solid line) and at 96 K (open circles).

takes place at 599, 582, 460, 200, and 130 K, respectively.<sup>9</sup> At 300 K, NdNiO<sub>3</sub> and PrNiO<sub>3</sub> are at the metallic state, whereas the other compounds are at the insulating state. For the insulators, a clear splitting is observed at the  $L_3$  edge ( $\sim 854$  eV), while for the metals this splitting is absent. Differences among spectra measured in the different electronic states are also noticeable at the  $L_2$  edge ( $\sim 872$  eV). PrNiO<sub>3</sub> and NdNiO<sub>3</sub> compounds spectra, measured at 96 K, when both are insulators, are analogous to those of  $R=Eu, Y,$  and  $Lu$  at 300 K, as shown by the splitting at the  $L_3$  edge for the PrNiO<sub>3</sub> compound (inset Fig. 1). Such modifications in the experimental spectra, unambiguously associated to the MI transition, demonstrate that important changes take place at the Ni local electronic structure. As the spectral shape depends mostly if the compound is metal or insulator, we conclude that the short-range scale electronic structure of all compounds shares a common basis.

To identify the electronic interactions accounting for the experimental data, charge transfer (configuration interaction) multiplet<sup>19,20</sup> (CTM) calculations were carried out. The calculations take into account interactions between three configurations,  $3d^7$ ,  $3d^8\bar{L}$ , and  $3d^9\bar{L}^2$ , in  $D_{4h}$  symmetry. A series of calculations varying the crystal field splitting parameter  $10D_q$ , keeping  $D_s=0.1$  eV,  $D_t=0.2$  eV fixed, is presented in Fig. 2. The configuration interaction parameters are  $\Delta=0.5$  eV,  $U_{dd}-U_{pd}=-1$  eV, and the transfer integrals  $T(B_1)=T(A_1)=2T(B_2)=2T(E)=2$  eV. The calculations matching the best with the experimental spectra for the metallic compounds are those with  $10D_q=2.2$  eV. The Ni<sup>3+</sup> metallic ground state turns out to be composed of 49%  $3d^7$  + 47%  $3d^8\bar{L}$  + 4%  $3d^9\bar{L}^2$ . The relative proportions for the three configurations are in reasonable agreement with those found by Mizokawa *et al.* for metallic PrNiO<sub>3</sub>.<sup>13</sup> The slight difference can be partially ascribed to the way the ligand hole is treated in the codes.<sup>21</sup> For the insulating compounds, a very good agreement with experiments is achieved by decreasing  $10D_q$  down to 2.0 or 1.9 eV. Such a decrease in  $10D_q$  leads to a less hybridized ground state composed of 61%  $3d^7$  + 37%  $3d^8\bar{L}$  + 2%  $3d^9\bar{L}^2$ .

Figure 3(a) shows the simulated spectrum for  $10D_q=1.9$  eV taking into account the  $l\cdot s$  coupling, as in Fig. 2(e),

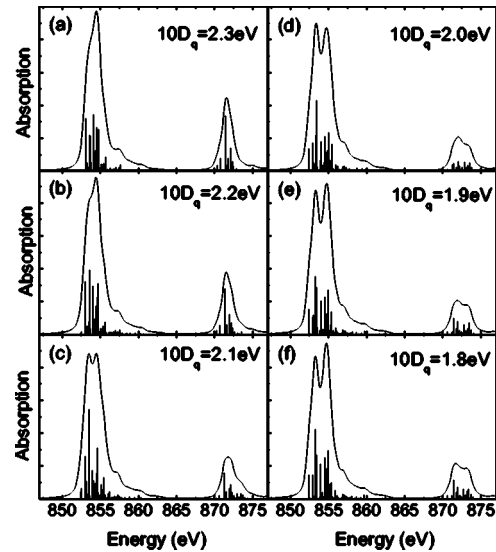


FIG. 2. CTM calculations of the Ni  $L$  XAS spectra in  $D_{4h}$  symmetry. The value of  $10D_q$  is varied between 2.3 eV (a) and 1.8 eV (f), in steps of 0.1 eV. The other parameters used are described in the text.

while Fig. 3(b) shows the calculation without the  $l\cdot s$  coupling. The effect on the spectral shape is remarkable. The ground state without the  $l\cdot s$  coupling is a HS state, schematically represented in Fig. 3(d). Figure 3(c) shows a calculation without the  $l\cdot s$  coupling, but where the initial state of the transition is the first excited state, which is a LS state, schematically represented in Fig. 3(e). The energy difference between these two states is found to be  $\sim 0.1$  eV. Since the  $l\cdot s$  coupling is of the same order, the insulating ground state turns out to be a mixing of LS and HS states. In addition, the calculation of the metallic state [Fig. 2(b)] is quite similar to that shown in Fig. 3(c), indicating that the LS state gives the main contribution to the metallic ground state. We conclude

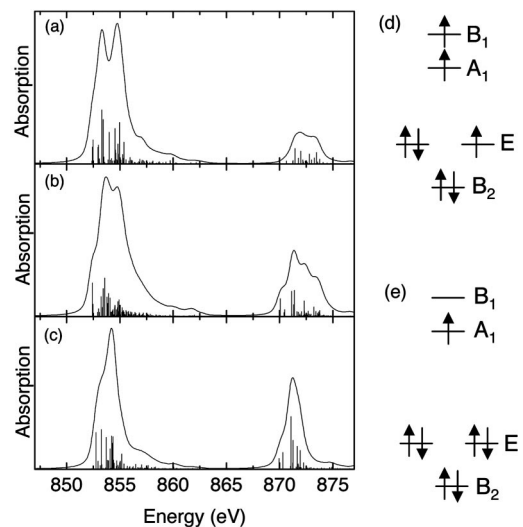


FIG. 3. CTM calculations for  $10D_q=1.9$  eV (a) with  $l\cdot s$  coupling, (b) without  $l\cdot s$  coupling, and (c) without  $l\cdot s$  coupling but with the initial state being the first excited state; (d) scheme of HS  $^4E$  and (e) LS  $^2A_1$  states.

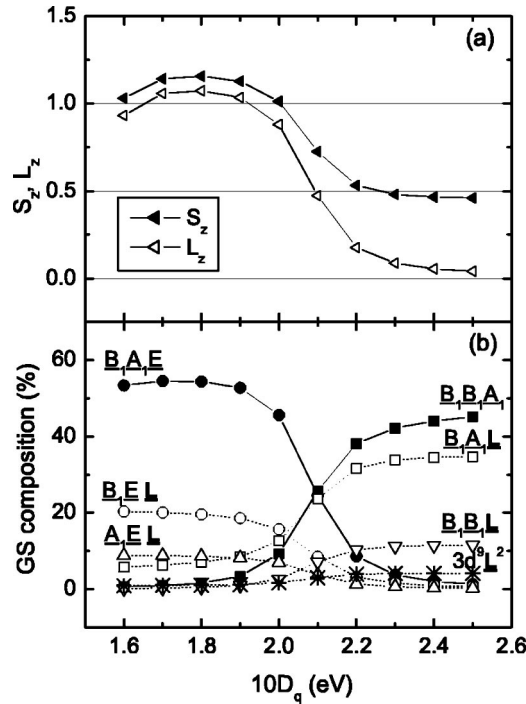


FIG. 4. (a) Variation of  $S_z$ ,  $L_z$  and (b) ground-state composition as a function of  $10D_q$ . The configuration  $\underline{B_1B_1A_1}$  corresponds to the LS  ${}^2A_1$  state in Fig. 3(e) and the configuration  $\underline{B_1A_1E}$  corresponds to the HS  ${}^4E$  state in Fig. 3(d). The others correspond to the charge transfer configurations.

that the ground state composition is very sensitive to the spin-orbit ( $l \cdot s$ ) coupling and that modifications in the crystal field splitting ( $10D_q$ ) change the relative contribution of both states to the mixed ground state.

The ground state (GS) can be decomposed into different symmetries that are mixed up by the  $l \cdot s$  coupling,

$$\begin{aligned} \Psi_{\text{GS}} = & \sum_{i;k+l+m+n=3} \alpha_i |a_1^k b_1^l b_2^m e^n\rangle \\ & + \sum_{j;k'+l'+m'+n'=2} \alpha_j |a_1^{k'} b_1^{l'} b_2^{m'} e^{n'} \underline{L}\rangle \\ & + \sum_{p;k''+l''+m''+n''=1} \alpha_p |a_1^{k''} b_1^{l''} b_2^{m''} e^{n''} \underline{L}^2\rangle. \end{aligned} \quad (1)$$

In this expression  $k+l+m+n$ ,  $k'+l'+m'+n'$ , and  $k''+l''+m''+n''$  are the number of  $d$  holes in  $3d^7$ ,  $3d^8 \underline{L}$ , and  $3d^9 \underline{L}^2$  configurations, respectively. The  $\alpha_i, \alpha_j, \alpha_p$  values can be obtained as described by Wasinger *et al.*<sup>22</sup> The contributions of these different symmetries to the ground state and to spin ( $S_z$ ) and orbital angular ( $L_z$ ) moments as functions of  $10D_q$  are shown in Fig. 4. The labels in Fig. 4(b) refer to the distribution of the  $d$  holes among  $B_1$ ,  $A_1$ ,  $B_2$ , and  $E$  orbitals. At the metallic state, with  $10D_q=2.2$  eV, the ground state is composed of  $\sim 38\%$   $\underline{B_1B_1A_1}$  (LS) and a small amount ( $\sim 8\%$ ) of  $\underline{B_1A_1E}$  (HS), the rest being charge transfer configurations. This leads to a net spin moment  $S_z \sim 0.5$ , in accordance with previous results that found a LS state for the metallic  $\text{PrNiO}_3$ .<sup>13</sup> Despite this strongly hybridized ground

state, the expected value for  $S_z$  is close to the  $\text{Ni}^{3+}$  LS ionic value. The reason is essentially due to the charge transfer configurations. The amount of charge transfer with spin up ( $S_z=1$  from  $\underline{B_1A_1L}$ ) is compensated by that of spin down ( $S_z=0$  from  $\underline{B_1B_1L}$ ). The ground-state transition takes place at  $10D_q=2.1$  eV, where we obtain the same contributions for HS and LS states, that is, the ground state is made of  $\sim 25\%$   $\underline{B_1A_1E}$  and of  $\sim 25\%$   $\underline{B_1B_1A_1}$ . The spin moment assumes an intermediate value  $S_z \sim 0.7$ . At the insulating state, with  $10D_q=2.0$  eV, the ground state is composed of  $\sim 46\%$   $\underline{B_1A_1E}$  (HS) and a small amount ( $\sim 9\%$ ) of  $\underline{B_1B_1A_1}$  (LS), the complement coming from charge transfer configurations. This leads to a net spin moment  $S_z \sim 1.0$ . The mixed-spin state arises because these compounds are between the strong and weak field limit and also due to the strong hybridization that mixes the Ni  $3d$  and O  $2p$  orbitals. In case there would be no charge transfer at all, the high- to low-spin transition would take place over a crystal field range of less than 0.1 eV. It is due to the strong covalence that there is a gradual change from the high- to low-spin ground state.

For the  $\underline{B_1B_1A_1}$  (LS) state, the electron coming from the O  $2p$  ligand band occupies the  $B_1$  orbital, even though it has a higher energy than  $A_1$ , owing to the gain in exchange energy. So,  $\underline{B_1A_1L}$  is the most important charge transfer configuration at the metallic state. On the other hand, for the  $\underline{B_1A_1E}$  (HS) state, the ligand electron must occupy an orbital already filled and there is no gain in exchange energy. In this case, the ligand electron occupies the  $A_1$  orbital, which is lower in energy than  $B_1$  and has a transfer integral twice larger than for the  $E$  orbital. Moreover, the  $\underline{B_1B_1A_1}$  (LS) state has all its three holes in orbitals that have strong mixing with the O  $2p$  ligand band ( $A_1$  and  $B_1$  come from the  $e_g$  orbital in  $O_h$  symmetry), whereas the  $\underline{B_1A_1E}$  (HS) state has a more localized hole in an  $E$  orbital that has less efficient overlap with the O  $2p$  ligand band. So, the increase of the HS component in the ground state and the decrease of the hybridization for smaller  $10D_q$  are related to each other.

The physical reason for a smaller  $10D_q$  at the insulating state originates in the coexistence of two nonequivalent Ni sites and overall increase of the average Ni-O bonding in all  $\text{RNiO}_3$  compounds.<sup>2,8,9</sup> Nonequivalent Ni sites coexist even at the metallic state<sup>11,12</sup> and are compatible with a segregation into two phases, where a more localized electron phase is embedded in a conducting background.<sup>23</sup> The MI transition takes place with the increase of the less hybridized phase related to the other. Alonso *et al.*<sup>8</sup> found for the heavier  $\text{RNiO}_3$  compounds, by refining neutron diffraction data in the monoclinic symmetry, an antiferromagnetic structure compatible with two nonequivalent moments. The smaller and larger Ni sites display magnetic moments of 0.7 and 1.4  $\mu_B$ , respectively. The values that we predict here for  $S_z$  are larger because the spin moments of the  $3d$  elements retain most of their isolated ion properties in x-ray absorption spectroscopy (XAS). Owing to the short time scale in XAS, essentially all electrons appear localized. Delocalized electrons should reduce these values in the solid. The same argument holds for the angular moment  $L_z$ , which is normally quenched in these compounds. Even if somewhat overestimated, our predictions show that an important parameter

controlling the properties of these compounds is the small splitting in distances, which leads to a different crystal field in each site. For the lighter  $RNiO_3$  powder compounds, the long-range structure has always been refined using a single Ni site and for that reason no such different spin values have been found. Recently, a monoclinic distortion was observed in thin films of  $NdNiO_3$ ,<sup>24</sup> questioning the orthorhombic symmetry obtained previously by neutrons. Our results show that the lighter and heavier  $RNiO_3$  compounds are very similar from the point of view of the local electronic structure. Experimental spectra look very similar and depend only if the compound is insulator or metal. So, we believe that the same physics observed in the heavier  $RNiO_3$  compounds may be involved in the lighter ones.

In conclusion, we presented experimental evidences of significant changes in the local electronic structure around  $Ni^{3+}$  in  $RNiO_3$  compounds. With the support of charge trans-

fer multiplet calculations, we showed that, concomitantly with the metal to insulator transition, a decrease of the crystal field splitting leads to a ground state transition from an essentially LS to a mixed-spin ground state. The mixed-spin ground state is possible because the energy separation between HS and LS states is of the same order of the spin-orbit coupling. The smaller hybridization, intrinsic to the HS state, gives an explanation to the more localized character at the insulating regime. The existence of a mixed-spin state, involving both LS and HS states and also charge transfer configurations, shed new light in the understanding of the unusual antiferromagnetic order observed below  $T_N$ , which is still an open question.

This work is partially supported by LNLS/ABTLuS. C.P. thanks FAPESP for support. A.Y.R. thanks CNPq for financial support as a visiting scientist.

- 
- <sup>1</sup>P. Lacorre, J. B. Torrance, J. Pannetier, A. I. Nazzal, P. W. Wang, and T. C. Huang, *J. Solid State Chem.* **91**, 225 (1991).
- <sup>2</sup>J. L. García-Muñoz, J. Rodríguez-Carvajal, P. Lacorre, and J. B. Torrance, *Phys. Rev. B* **46**, 4414 (1992).
- <sup>3</sup>J. B. Torrance, P. Lacorre, A. I. Nazzal, E. J. Ansaldo, and C. Niedermayer, *Phys. Rev. B* **45**, R8209 (1992).
- <sup>4</sup>N. E. Massa, J. A. Alonso, M. J. Martínez-Lope, and I. Rasines, *Phys. Rev. B* **56**, 986 (1997).
- <sup>5</sup>M. Medarde, P. Lacorre, K. Conder, F. Fauth, and A. Furrer, *Phys. Rev. Lett.* **80**, 2397 (1998).
- <sup>6</sup>J. L. García-Muñoz, J. Rodríguez-Carvajal, and P. Lacorre, *Phys. Rev. B* **50**, 978 (1994).
- <sup>7</sup>J. Rodríguez-Carvajal, S. Rosenkranz, M. Medarde, P. Lacorre, M. T. Fernández-Díaz, F. Fauth, and V. Trounov, *Phys. Rev. B* **57**, 456 (1998).
- <sup>8</sup>J. A. Alonso, J. L. García-Muñoz, M. T. Fernández-Díaz, M. A. G. Aranda, M. J. Martínez-Lope, and M. T. Casais, *Phys. Rev. Lett.* **82**, 3871 (1999).
- <sup>9</sup>J. A. Alonso, M. J. Martínez-Lope, M. T. Casais, J. L. García-Muñoz, and M. T. Fernández-Díaz, *Phys. Rev. B* **61**, 1756 (2000).
- <sup>10</sup>F. de la Cruz, C. Piamonteze, N. E. Massa, H. Salva, J. A. Alonso, M. J. Martínez-Lope, and M. T. Casais, *Phys. Rev. B* **66**, 153104 (2002).
- <sup>11</sup>C. Piamonteze, H. C. Tolentino, A. Y. Ramos, N. E. Massa, J. A. Alonso, M. J. Martínez-Lope, and M. T. Casais, *Phys. Scr.* (to be published).
- <sup>12</sup>C. Piamonteze, H. C. Tolentino, A. Y. Ramos, N. E. Massa, J. A. Alonso, M. J. Martínez-Lope, and M. T. Casais, *Phys. Rev. B.* (to be published).
- <sup>13</sup>T. Mizokawa, A. Fujimori, T. Arima, Y. Tokura, N. Möri, and J. Akimitsu, *Phys. Rev. B* **52**, 13865 (1995).
- <sup>14</sup>T. Mizokawa, D. I. Khomskii, and G. A. Sawatzky, *Phys. Rev. B* **61**, 11263 (2000).
- <sup>15</sup>C. Piamonteze, H. C. Tolentino, F. C. Vicentin, A. Y. Ramos, N. E. Massa, J. A. Alonso, M. J. Martínez-Lope, and M. T. Casais, *Surf. Rev. Lett.* **9**, 1121 (2002).
- <sup>16</sup>Z. Hu *et al.*, *Phys. Rev. Lett.* **92**, 207402 (2004).
- <sup>17</sup>I. A. Nekrasov, S. V. Streltsov, M. A. Korotia, and V. I. Anisimov, *Phys. Rev. B* **68**, 235113 (2003).
- <sup>18</sup>J. A. Alonso, M. J. Martínez-Lope, and I. Rasines, *J. Solid State Chem.* **120**, 170 (1995).
- <sup>19</sup>F. M. F. de Groot, *J. Electron Spectrosc. Relat. Phenom.* **67**, 529 (1994).
- <sup>20</sup>F. M. F. de Groot, *Coord. Chem. Rev.* **249**, 31 (2005).
- <sup>21</sup>The multiplet program used considers the ligand hole as having  $d$  symmetry, whereas cluster programs take into account the real  $p$ -ligand states.
- <sup>22</sup>E. C. Wasinger, F. M. F. de Groot, B. Hedman, K. O. Hodgson, and E. I. Solomon, *J. Am. Chem. Soc.* **125**, 12894 (2003).
- <sup>23</sup>J.-S. Zhou, J. B. Goodenough, B. Dabrowski, P. W. Klamut, and Z. Bukowski, *Phys. Rev. B* **61**, 4401 (2000).
- <sup>24</sup>U. Staub, G. I. Meijer, F. Fauth, R. Allenspach, J. G. Bednorz, J. Karpinski, S. M. Kazadov, L. Paolasini, and F. d'Acapito, *Phys. Rev. Lett.* **88**, 126402 (2002).